Coupled Macromolecular Transport and Gel Mechanics: Poroviscoelastic Approach

P. A. Netti and F. Travascio
Dept. of Materials and Production Engineering, University of Naples Federico II, 80125 Naples, Italy

R. K. Jain
Dept. of Radiation Oncology, Harvard Medical School and Massachusetts General Hospital, Boston, MA 02114

Designing drug delivery devices or drug delivery protocols poses problems because they are considered to operate in a mechanically static environment. It should consider, however, transport processes in these cases occur in a mechanically dynamic environment since mechanical stimuli may strongly influence transport within soft hydrated materials. A general framework combines fluid and macromolecular transport with the mechanics of hydrated polymer gels or tissue. As an example, the model equations have been created for a spherical geometry to describe the distribution of macromolecules within the gel resulting from a constant pressure or a constant flow infusion source. The model describes the overall average profiles of the interstitial fluid pressure, velocity and solid matrix dilatation, displacement, and stress, as well as macromolecular distribution. The basic theory provides new insight into understanding the transport of macromolecules within mechanically stimulated polymeric gels and tissues and, therefore, represents a valuable tool for designing and engineering novel drug delivery systems, as well as optimization of drug delivery protocols to be used in detection and treatments.

Introduction

Polymeric gels are widely used as drug carriers and drug delivery devices in many biotechnological applications, such as tissue engineering, and tissue and organ regeneration *in vivo* (Shea et al., 1999; Baldwin and Saltzman, 1998; Jen et al., 1996; Muhr and Blonshard, 1982). For all of these applications, the gel has to be engineered in such a way that a specific biologically active molecule is delivered by the material according to a specific release time sequence. However, a problem with the design of such devices is that they are generally thought to operate under mechanically static conditions, whereas in reality they have to perform under complex stress conditions, often variable with time. Since the transport of macromolecules within polymeric gels is part of the dynamic equilibrium among matrix deformation, fluid pressure, and interstitial velocity, the role of the mechanical environment on the delivery mechanism cannot be neglected. In principle, since matrix deformation can lead to the convective transport of macromolecules, transient macromolecular fluxes can be induced in the physical domain by a simple mechanical stimulation even in the absence of concentration gradients. For instance, periodic mechanical loading enhances the efficiency of delivering macromolecules from a polymer gel (Lee et al., 2000).

A polymeric gel is a biphasic system composed of a solid network embedded in a fluid phase. The equilibrium of the system is reached when the forces acting on the fluid phase, mainly hydrostatic and osmotic pressures, balance the elastic response of the polymeric chains (Flory, 1992). Each perturbation of the equilibrium state generates both a network deformation and a fluid redistribution. Two mathematical models, mixture theory and poroelasticity, have been used in the literature to describe the elastodynamics of gel systems. These approaches couple the deformation of the polymer network and the transport of fluid occurring within it. The first model, which describes a gel-like mixture of a solid and a fluid phase, has been introduced by Truesdell and Toupin (1960) and by Mow et al. (1980) to study the behavior of biological tissues, and more recently to describe polymer solutions and gels (Ianniruberto et al., 1994; Doi, 1996). The second, formerly introduced by Biot (1941, 1955), considers the system made

Correspondence concerning this article should be addressed to P. A. Netti.

up by a solid poroelastic matrix, similar to a sponge, saturated by the fluid. This model has been extended to describe the behavior of gels and biological tissues (Mak, 1986). These studies demonstrated how the fluid transport mechanism plays an important role in determining the macroscopic mechanical behavior of these systems, both in static (Mow et al., 1980) and in dynamic (Frank and Grodzinsky, 1987) regimes.

The aim of this work is to investigate the role of mechanical stress and deformation on fluid and macromolecular distribution within a gel. To this end we have adopted the previous models to describe the fluid transport within a polymer gel by using a customized viscoelastic constitutive equation for the solid network. The equations just mentioned, along with an appropriate diffusive convective equation, are able to describe the influence of the deformation of the polymer network on the macromolecular distribution. As a specific example, the equations have been specialized for a spherical geometry to describe the distribution of macromolecules within the gel resulting from an infusion by a constant pressure or a constant flow source. The model describes the overall average profiles of the interstitial fluid pressure, velocity, and solid matrix dilatation, displacement, and stress, as well as macromolecular distribution.

The scope of this specific application is to simulate an intratumoral infusion, due to the high relevance of this topic in cancer therapy. In this case, the mechanical stimuli are provided by the infusing source. Comparing the results of the present model with those obtainable with a rigid porous model, it is concluded that the poroviscoelastic approach not only allows the description of transient evolution but it also provides information on the stress distribution within the tissue, which may be a key factor in enhancing and improving the delivery of macromolecular medicine in solid tumors. The analysis performed helps in designing intratumoral infusion protocols.

The analysis of more complex mechanical environments acting on the material would provide further information about the mechanical stimulation effects on the macromolecular distribution within a gel system (Lee et al., 2000) and will be presented in a future article.

Mathematical Model

Assuming that a polymeric gel, which is a biphasic system constituted by a solid network and a fluid phase, is a homogeneous and isotropic medium, each variable and parameter is to be meant as an average over a scale of several gel pores or mesh sizes. If ζ is the generic variable or parameter and δV is the elementary volume, the average value of ζ is expressed by the following relationship

$$\langle \zeta \rangle = \frac{\int_{\delta V} \zeta \, \delta V}{\delta V} \tag{1}$$

Macromolecular movement within a polymer gel may be driven by the concentration gradient (diffusion) or by interstitial fluid velocity (convection). To describe interstitial fluid velocity within the gel we followed a previously developed model to describe fluid movement in solid tumors with capillary resorption (Netti et al., 1997), extending it to take into account the effect of the viscoelastic nature of the polymeric gel. In the following section, the governing equations for fluid transport and gel mechanics are presented along with a convection–diffusion equation to describe the distribution of macromolecules within the system.

It should be emphasized that this model, based on the biphasic theory, is applicable to both *macroscopically* porous gels and to highly entangled polymer solutions or gels. In the former case, the fluid phase is present within macroscopically porous gels, such as fibrillar gels or tissues (agarose gel, collagen, extracellular matrix, and so on), as a distinct phase within the porosity (Netti et al., 2000). In these systems, external mechanical stimuli may lead to a convective fluid transport due to a nonbalanced hydrostatic pressure gradient. On the other hand, when an external stress field is applied to an entangled polymer solution or gel, an osmotic pressure gradient will arise to balance the solvatation and the elastic forces of the polymeric network (Flory, 1992; Ianniruberto et al., 1994; Doi and Edwards, 1986). Therefore, there will be convective fluid flows associated with osmotic pressure gradients in a similar fashion to those occurring in macroscopically porous gels related to hydrostatic pressure gradients. In both cases, the mathematical formulation of the coupling of the mechanics and transport is given by a generalized Darcy's Law (Doi, 1996).

We adopted a formulation typical of macroscopically porous gels, for the coupling of fluid motion and elastic response of the solid network, from the specific application to which the model will be applied in the next section (intratumoral infusions).

Governing equations for fluid transport

Mass Balance. Hereafter we will adopt the following nomenclature: $\boldsymbol{v}$ and $\boldsymbol{u}$ are the fluid velocity and the displacement of the solid matrix, respectively; φ is the volumetric fraction of the fluid phase; ρ_f and ρ_s are the density of fluid and solid phases, respectively. Assuming that the solid and fluid phases have the same specific volume ($\rho_s/(1-\varphi) = \rho_f/\varphi$), the mass balances for the fluid and solid phase can be written as

$$\frac{\partial \varphi}{\partial t} = -\nabla \cdot \varphi \boldsymbol{v}$$

$$\frac{\partial (1-\varphi)}{\partial t} = \nabla \cdot \left[(1-\varphi) \frac{\partial}{\partial t} \underline{\boldsymbol{u}} \right] \tag{2}$$

Summing up the preceding equations, the mass balance for the solid–fluid system can be written as

$$\nabla \cdot \left[\varphi \boldsymbol{v} + (1-\varphi) \frac{\partial}{\partial t} \boldsymbol{u} \right] = 0 \tag{3}$$

In writing these equations we assumed that neither generation nor absorption terms are present.

Momentum Balance. Assuming that body and inertial forces are negligible, the momentum balance on the fluid and

solid phases can be written as (Mow et al., 1986)

$$\nabla \cdot \underline{\underline{\sigma}}^{f} = \mathbf{\Pi}$$

$$\nabla \cdot \underline{\underline{\sigma}}^{s} = -\mathbf{\Pi} \tag{4}$$

where $\underline{\underline{\sigma}}^{f}$ and $\underline{\underline{\sigma}}^{s}$ are the total stress (Terzaghi tensor) in the fluid and solid phase, respectively. The term $\mathbf{\Pi}$ is the sum of the external forces acting on the single phase, and can be expressed as (Ateshian et al., 1997)

$$\mathbf{\Pi} = \boldsymbol{F}_a + p\nabla(1-\varphi) \tag{5}$$

where F_a is the frictional force exerted by the fluid on the solid matrix due to their relative motion; under the hypothesis of slow motion, it can be expressed as

$$\boldsymbol{F}_a = \left[\boldsymbol{v} - \frac{\partial}{\partial t}\boldsymbol{u}\right] f \tag{6}$$

where f is the friction coefficient. The second term on the righthand side in Eq. 5 shows that a gradient of the fluid volumetric fraction leads to the development of a pressure force on the solid phase.

From the preceding equations, the total momentum balance for the solid–fluid system can be written as

$$\nabla \cdot \underline{\underline{\sigma}}^{f} + \nabla \cdot \underline{\underline{\sigma}}^{s} = 0 \tag{7}$$

Constitutive Equation. The linear biphasic theory (Mow et al., 1980) considers the solid matrix as a linear elastic solid, and, thus, the time-dependent effects of the system are only due to fluid redistribution within the solid matrix. Here, to better describe the real rheological and mechanical behavior of polymeric gels, we adopted a specially defined viscoelastic constitutive equation for the gel. The introduction of viscoelasticity brings about additional time-dependent effects due to the configurational relaxation of the polymer chains. To formulate a constitutive equation for the solid phase, we invoke the Boltzmann's superposition principle, assuming that the mechanical behavior of the gel can be described as the sum of a linear viscoelastic and a linear-elastic contribution. The viscoelastic contribution is described by a memory function of the material (Macosko, 1994), while the elastic response is taken into account by introducing the Lamè constants. The constitutive equation for the solid stress tensor is then

$$\underline{\underline{\sigma}}^{s} = \underbrace{-(1-\varphi)p\underline{\underline{I}}}_{\text{hydrostatic}} + \underbrace{2\mu\underline{\underline{\epsilon}} + \lambda e\underline{\underline{I}}}_{\text{elastic}} + \underbrace{c\int_{-\infty}^{t} m(t-\xi)\frac{\partial}{\partial \xi}\left(\underline{\underline{\epsilon}} + e\underline{\underline{I}}\right)d\xi}_{\text{viscoelastic}} \tag{8}$$

In this expression $\underline{\underline{\epsilon}}$ is the deformation tensor, and e is the dilatation of the solid matrix [$e = tr(\underline{\underline{\epsilon}})$]; μ and λ are the Lamè constants, while $m(t)$, c, and τ are the memory function, a viscoelastic constant characteristic of the material, and the mean relaxation time, respectively. We defined a unique memory function to describe the response of the system both for e and $\underline{\underline{\epsilon}}$. It could be argued that the relaxation of the deformation can be different from that of volumetric dilatation, since different mechanisms of chain relaxation may be involved. However, the definition of a different memory function to describe the relaxation of e and $\underline{\underline{\epsilon}}$ would introduce three more material parameters making the analysis of the model more elaborate and well beyond the scope of this study.

The memory function can be expressed in terms of the spectrum of relaxation times as (Macosko, 1994)

$$m(t) = \int_0^{\infty} \frac{H(\xi)}{\xi} e^{-t/\xi} d\xi \tag{9}$$

The spectrum of the relaxation times $H(\phi)$ has been arbitrarily assumed as

$$H(\xi) = \frac{\tau}{\delta} \qquad \forall \phi \in [\tau - \delta, \tau + \delta]$$

$$H(\xi) = 0 \qquad \forall \phi \notin [\tau - \delta, \tau + \delta] \tag{10}$$

where $\tau + \delta$ and $\tau - \delta$ are the shortest and the longest relaxation times, respectively. The parameter δ measures the semiamplitude of the spectrum of the relaxation times. The assumption of this expression for the spectrum of relaxation times is based on the capability of this expression to describe qualitatively the dynamic mechanical data of polymer gels that show a weak dependence of the viscous modulus G'' upon the frequency (Fung, 1990). The preceding expression, $m(t)$, makes the integral term of Eq. 9 yield the usual expression of a Lodge fluid when the system has only one relaxation time.

To define the constitutive equation for the fluid phase, it should be pointed out that the velocity $\boldsymbol{v}$ considered here is the average velocity through the gel network and not the local velocity within the single pore. This velocity field can be assumed to be conservative (Netti et al., 1997), and, hence, the contribution of the fluid to the total stress tensor can be expressed as

$$\underline{\underline{\sigma}}^{f} = -\varphi p\underline{\underline{I}} \tag{11}$$

where p is the hydrostatic pressure.

Combining Eqs. 11, 4 and 5, the momentum balance on the fluid phase can be rewritten as

$$\varphi\left[\boldsymbol{v} - \frac{\partial}{\partial t}\boldsymbol{u}\right] = -K\nabla p \tag{12}$$

where K is the average material hydraulic permeability. This relation can be regarded as a generalized version of Darcy's law, and expresses the coupling between fluid motion and matrix displacement. Equation 12 reveals clearly the biphasic nature of a polymer gel. Not only a gradient of hydrostatic pressure induces a fluid flow and solid matrix displacement but also a solid matrix displacement may, in turn, lead to a hydrostatic pressure gradient and fluid flow.

Macromolecular transport

In general, the solute transport within a polymer gel can occur by both diffusion and convection. The diffusive flux, N_d, can be expressed in general terms as

$$\boldsymbol{N}_d = -D\boldsymbol{\nabla}C \tag{13}$$

where D is the diffusion coefficient of the solute in the gel system, while C is the average mass concentration of solute in the gel. Under the hypothesis of small deformation, D can be assumed to be constant and independent of the deformation of the solid matrix. The solute concentration, C, depends upon the deformation state of the solid matrix and this should be taken into account for a rigorous description of the diffusive transport. The solute concentration C varies with the gel deformation according to the equation

$$C = C_o \frac{V_o^f}{V^f} \tag{14}$$

where C_o is the mass concentration in the undeformed state, and V^f and are V_o^f the fluid volumes in the deformed and undeformed state, respectively. From the definition of gel dilatation under the hypothesis of small deformation, we have

$$\epsilon \cong \frac{\delta V_f}{V_o} = \frac{V^f - V_o^f}{V_o} \tag{15}$$

where V_o is the undeformed volume of the gel. From this equation, the concentration of a solute within a deformed gel can be expressed as

$$C = C_o \left(\frac{1}{1 + \dfrac{e}{\varphi_o}} \right) \tag{16}$$

where φ_o is the initial volumetric fraction of the fluid phase. If the deformations are very small, that is $(e/\varphi_o \ll 1)$, then $C \approx C_o$.

The solute convective flux, $\boldsymbol{N}_c$, can be expressed as

$$\boldsymbol{N}_c = C\chi\boldsymbol{v} \tag{17}$$

The screening coefficient χ is a measure of the relative velocity between the solute and the fluid, and is defined as the ratio of the average solute-to-fluid velocity. According to

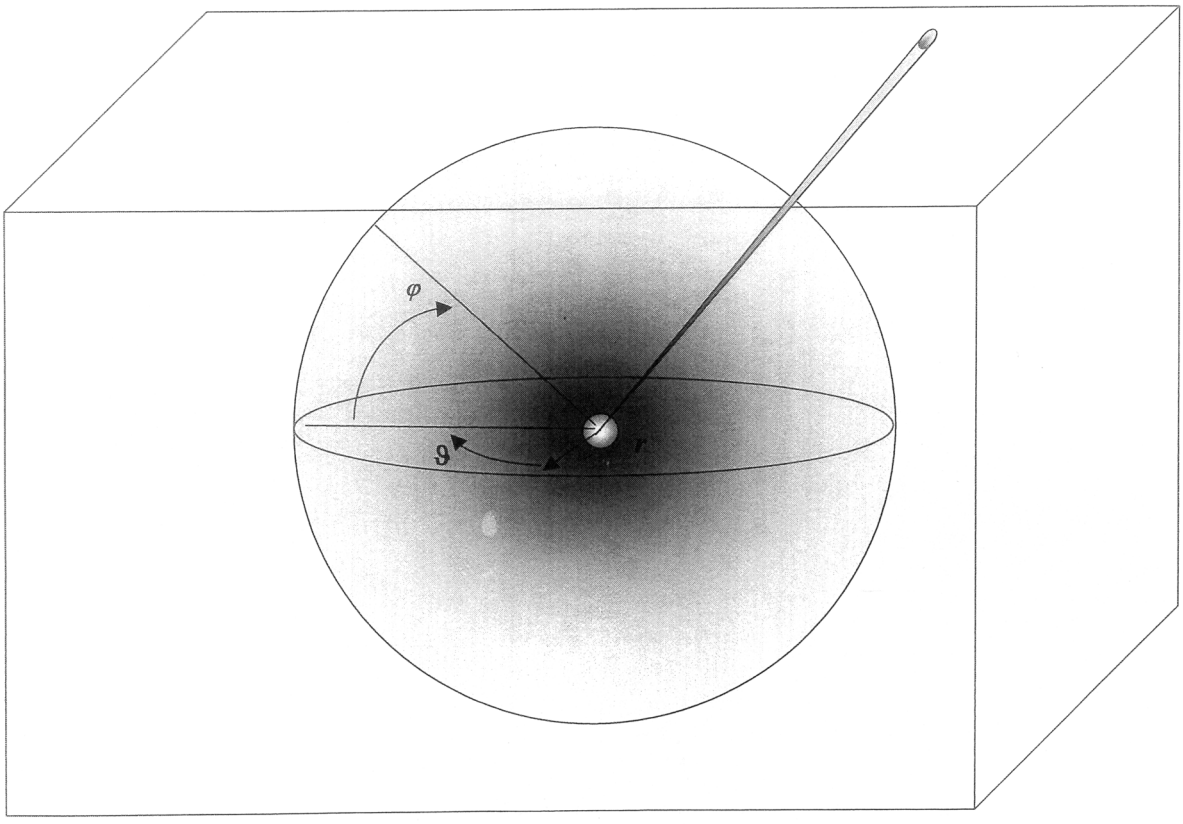

Figure 1. Intragel infusion.

A core of radius a is carved out from the central part of the gel. The fluid pressure and the fluid flow are assumed to be constant within the region of radius a.

Johnson and Deen (1999), this factor depends upon the hydrodynamic radius of the solute, its charge as well as the properties of the gel, and may assume values either greater or smaller than unity.

Given the constitutive equations for the diffusive and convective fluxes, the solute balance can be written as

$$\frac{\partial C}{\partial t} = D\nabla^2 C - \nabla\cdot(C\chi \boldsymbol{v}) \tag{18}$$

The system of Eqs. 3, 7, 12, and 18, together with the boundary conditions, describe the mechanics of the fluid and macromolecular transport in gel systems.

In the following section, as an example, the preceding equations will be specialized to the case of a spherical geometry.

Application to an axisymmetric geometry

Here, the model described in the previous section will be used to study the transport of macromolecules within a polymeric gel infused with a constant pressure or constant flow point source. The physical domain is assumed to be spherical, in which a solution of a macromolecular solute is infused from a small region of diameter a carved out from the gel (see Figure 1). For the particular choice of the geometry, the problem is unidimensional. However, the particular choice of the geometry is not as limiting as it may seem. Indeed, if we consider a generic body, whose greatest dimension is large enough compared to the internal cavity diameter, both pressure, velocity, dilatation, stress, and concentration profiles evolve, as in a spherical domain, around an area sufficiently close to the cavity (Figure 1). Therefore, calculations on a hollow spherical system furnish a first approximation for a more general domain.

For axisymmetric domains, with r the radial coordinate, the deformation tensor is

$$\underline{\underline{\epsilon}} = \begin{pmatrix} \dfrac{\partial u_r}{\partial r} & 0 & 0 \\ 0 & \dfrac{u_r}{r} & 0 \\ 0 & 0 & \dfrac{u_r}{r} \end{pmatrix} \tag{19}$$

and, therefore, the dilatation, e, can be expressed as

$$e = tr(\underline{\underline{\epsilon}}) = \frac{\partial u_r}{\partial r} + 2\frac{u_r}{r} \tag{20}$$

By combining Eqs. 3, 7, and 12, the gel mechanics can be expressed by the following integrodifferential equation in e (see the Appendix)

$$\frac{\partial e}{\partial t} = K(\lambda + 2\mu)\frac{1}{r^2}\frac{\partial}{\partial r}\left(r^2\frac{\partial e}{\partial r}\right) + 2cK\int_{-\infty}^{t} m(t-\xi)\frac{\partial}{\partial \xi}\left[\frac{1}{r^2}\frac{\partial}{\partial r}\left(r^2\frac{\partial e}{\partial r}\right)\right] d\xi \tag{21}$$

which, transformed in the Laplace space, becomes

$$s\hat{e}(s,r) = K\left[(\lambda + 2\mu) + \frac{2c\tau}{\delta}\ln\left(\frac{s(\tau+\delta)+1}{s(\tau-\delta)+1}\right)\right]\nabla^2\hat{e}(s,r) \tag{22}$$

Equation 22 is mathematically similar to that describing anomalous diffusion in the polymeric system. Indeed, the multiplying coefficient of the Laplacian can be seen as a time-dependent pseudodiffusion coefficient, similar to the time-dependent diffusion coefficient defined to describe anomalous diffusion in swelling polymers (Del Nobile et al., 1994). According to this analogy, Eq. 22 states that the transient fluid redistribution within a gel is regulated by the mechanism of fluid percolation through the polymer network, controlled by K, and by the relaxation time of polymer chains, controlled by τ. Equation 22 can be solved in the Laplace space to find the temporal and spatial evolution of the solid matrix dilatation (see the Appendix).

In the following we will consider two particular cases of infusion: (1) constant pressure and (2) constant flow infusion.

1. In the case of constant pressure infusion, the pressure in the internal cavity is constant and equal to PI, the infusion pressure. If the external radius of the sphere, R, is sufficiently large compared to the internal one, $R/a \gg 1$, we can assume that the dilatation e vanishes at $r \to R$ hence

$$\begin{aligned} p &= PI \qquad \text{for} \quad r = a \\ e &= 0 \qquad \text{for} \quad r = R \end{aligned} \tag{23}$$

2. In the case of constant flow infusion, the solution is infused into the cavity at a rate equal to Q. If the external radius is sufficiently large compared to the internal one, $R/a \gg 1$, that the dilatation e vanishes at $r \to R$, hence

$$\begin{aligned} v &= \frac{Q}{r\pi a^2} \qquad \text{for} \quad r = a \\ e &= 0 \qquad \text{for} \quad r = R \end{aligned} \tag{24}$$

For the two cases just considered it is possible to find an analytical expression of the dilatation in the Laplace space (see the Appendix)

$$\hat{e}(s,r) = \frac{D(s)a}{r}\frac{\sinh[(R-r)\alpha]}{\sinh[(R-a)\alpha]} \tag{25}$$

$$\hat{e}(s,r) = \frac{D'(s)a^2}{r} \times \frac{\sinh[(R-r)\alpha]}{(1-C(s)a)\sinh[(R-a)\alpha] + \alpha a\cosh[(R-a)\alpha]} \tag{26}$$

where $D(s)$, $D'(s)$ and $C(s)$ are complex coefficients expressed in terms of the characteristic parameters of the material. Once the distribution of $\hat{e}$ is known, all the other variables $\hat{p}$, $\hat{u}$, $\hat{v}$, and $\hat{\sigma}$ are readily obtained (see the Appendix for details).

The distribution of macromolecules can be obtained from Eq. 18. Due to the complexity of the fluid-velocity field, the integration of Eq. 18 has been carried out through a finite-element scheme, assuming the following boundary conditions (see the Appendix for details)

$$\begin{aligned} C &= C^i \quad \text{for} \quad r = a \quad \forall t \\ C &= 0 \quad \text{for} \quad r = R \quad \forall t \\ C &= 0 \quad \text{for} \quad t = 0 \quad \forall r \in]a, R[\end{aligned} \tag{27}$$

where C^i is the concentration of macromolecules within the gel, not to be confused with the concentration of macromolecules of the fluid contained in the cavity, C^*. The concentration C^* is related to C^i by means of the solubility coefficient ϕ, $C^i = \phi C^*$.

Results

The spatial and temporal evolutions of the average hydrostatic fluid pressure and velocity, matrix dilatation, and solid stress are calculated by Eqs. A24, A30, A14, A23, A34, and A35 in Appendix A, using the quotient difference method for the numerical inversion of the Laplace transform (Hoog et al., 1982). For the simulations the ratio a/R has been assumed to be much less than unity (= 0.035) and the parameters K, c, λ, μ, τ, and D have been taken from the literature (see Table 1) and assumed to be constant.

The transient process is controlled by two characteristic times, namely relaxation and percolation. Relaxation time, τ, represents the characteristic times for polymer chain rearrangements, while percolation time measures the time for fluid redistribution within the network and is given by

$$T_{\text{percolation}} = \frac{4\pi R^2}{K(\lambda + 2\mu)} \tag{28}$$

Constant pressure infusion

Steady State. The steady-state analytical expressions of matrix dilatation, fluid pressure, and velocity and radial stress are as follows

$$e_{ss}(r) = \frac{PI \cdot a}{(a-R)(\lambda+2\mu)}\left(1 - \frac{R}{r}\right) \tag{29}$$

$$p_{ss}(r) = \frac{PI \cdot a}{(a-R)}\left(1 - \frac{R}{r}\right) \tag{30}$$

$$v_{ss}(r) = \frac{PI \cdot Ka}{(R-a)\varphi}\frac{R}{r^2} \tag{31}$$

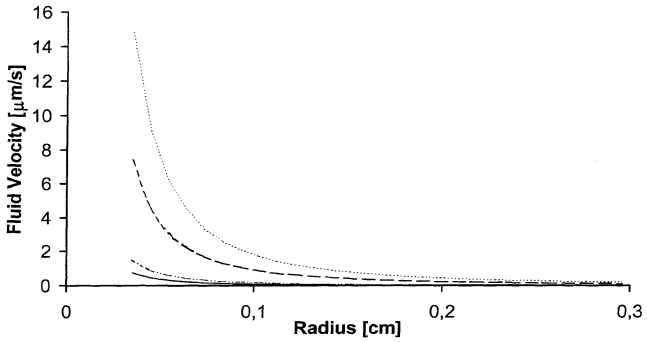

Figure 2. Steady-state fluid-velocity profile for a constant pressure infusion at 1.3 kPa.

(. . .) $K = 7.6\times10^{-10}$ m^2/kPa·s; (– –) $K = 3.8\times10^{-10}$ m^2/kPa·s; (–·–) $K = 7.6\times10^{-11}$ m^2/kPa·s; (_) $K = 3.8\times10^{-11}$ m^2/kPa·s.

The pressure profile is controlled only by the infusion pressure, while the fluid velocity and the matrix dilatation depend upon the material properties. The matrix dilatation depends on the elastic modulus, while the velocity profile depends on the hydraulic conductivity of the matrix, as shown in Figure 2. The magnitude of the fluid-velocity field increases with the value of K. Having assumed the material properties to be constant, the expression for the pressure and the fluid velocity are the same, as for infusion in a rigid porous material (Morrison et al., 1994).

Transient Process. The transient process is influenced by the fluid transport properties of the matrix (K) and by its mechanical properties (λ, μ, c, and τ). The first three parameters modulate the percolation time, while the others are related to the viscoelastic contribution. The effect of the hy-

Table 1. Transport and Mechanical Parameters

Parameter	Value	Unit	Reference
Q	0.1–10	mm^3/min	
PI	0.65–2.6	kPa	
R	1	cm	
a	0.035	cm	
C_o	0.5	g/cm^3	
χ	1	Dimensionless	
D	1×10^{-8}–1×10^{-6}	cm^2/s	Morrison et al. (1994); Jain (1987); Netti et al. (1997)
λ	13.16	kPa	Netti et al. (1997); Nicholson and Phillips (1981)
μ	6.58	kPa	Nicholson and Phillips (1981)
c	0–52	kPa	
τ	300	s	Netti et al. (1997)
ϕ	0.2	Dimensionless	Jain (1987)
K	7.6×10^{-12}–7.6×10^{-16}	m^2/kPa·s	Jain (1987); Boucher et al. (1998); Johnson and Deen (1996); Swabb et al. (1974)

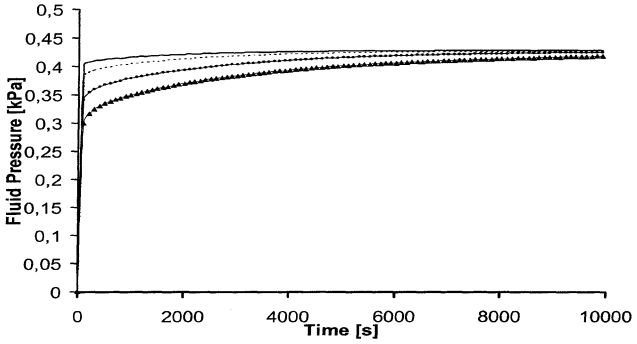

Figure 3. Transient fluid-pressure profile for a constant pressure infusion at 1.3 kPa as a function of the hydraulic conductivity of the matrix.

(_) $K = 7.6 \times 10^{-10}$ m^2/kPa·s; (. . .) $K = 3.8 \times 10^{-10}$ m^2/kPa·s; (–·–) $K = 7.6 \times 10^{-11}$ m^2/kPa·s; (▲) $K = 3.8 \times 10^{-11}$ m^2/kPa·s.

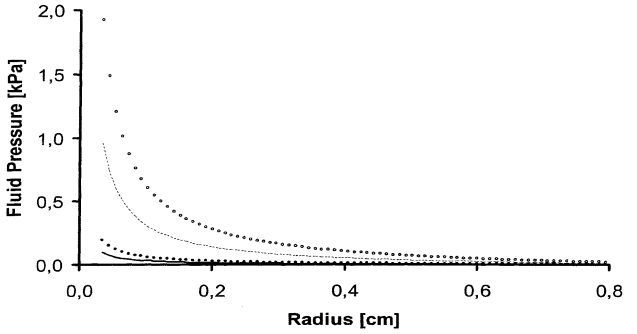

Figure 5. Steady-state fluid-pressure profile for a constant flow infusion at 0.1 μL/min as a function of the hydraulic conductivity of the matrix.

(_) $K = 7.6 \times 10^{-10}$ m^2/kPa·s; (●) $K = 3.8 \times 10^{-10}$ m^2/kPa·s; (– –) $K = 7.6 \times 10^{-11}$ m^2/kPa·s; (○) $K = 3.8 \times 10^{-11}$ m^2/kPa·s.

draulic permeability upon the evolution of the fluid-pressure profile is shown in Figure 3. As expected, increasing K results in a faster evolution of the pressure profile toward equilibrium. The elastic moduli of the polymer network (λ and μ) play a similar role in the time evolution of the fluid-pressure profile (data not shown). The viscoelastic modulus, c, also contributes to a reduction in the time scale of the transient process, albeit its effect fades for times longer than the relaxation time (τ), as shown in Figure 4. The solid line represents the pressure profile of a poroelastic system ($c = 0$). As c increases, the pressure increases and the time for fluid redistribution decreases. However, these effects are only present for times less then the viscoelastic relaxation time; at longer times, the poroviscoelastic curves fall onto that of a poroelastic material.

Constant flow infusion

Steady State. The steady-state expressions of matrix dilatation, fluid pressure, and velocity and radial stress are as follows

$$e_{ss}(r) = \frac{\varphi Q}{4K\pi R(\lambda + 2\mu)}\left(1 - \frac{R}{r}\right) \tag{32}$$

$$p_{ss}(r) = \frac{\varphi Q}{4K\pi R}\left(1 - \frac{R}{r}\right) \tag{33}$$

$$v_{ss}(r) = \frac{Q}{4\pi r^2} \tag{34}$$

When the fluid is infused at constant flow, the fluid redistribution at the steady state depends upon the fluid transport properties of the gel (K). For this reason, contrary to the case of constant pressure infusion, the fluid-pressure profile is controlled by the hydraulic permeability, while the velocity profile does not depend upon the material properties. Figure 5 shows the influence of K on the pressure profile; as K decreases the pressure profile increases.

Transient Process. As in the case of constant pressure infusion, the transient process is influenced by the fluid transport properties of the matrix (K) and by its mechanical properties (λ, μ, c, and τ). The last two parameters (c and τ) modulate the time response of the system during the transient; the higher the modulus c, the shorter the transient in the fluid-pressure profile evolution, as shown in Figure 6. However, the effect of c on the pressure profile is short lived,

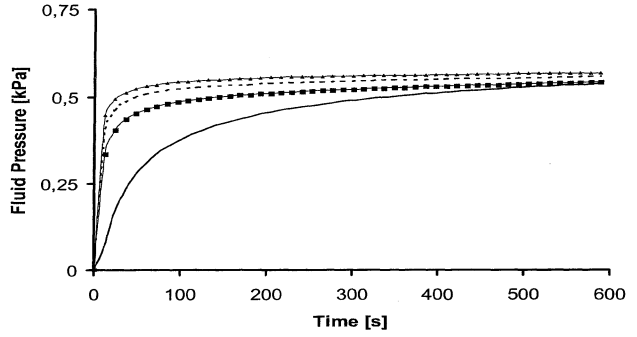

Figure 4. Transient fluid-pressure profile for a constant pressure infusion of 1.3 kPa parametric with the viscoelastic modulus c.

(–▲–) $c = 52$ kPa; (– –) $c = 26$ kPa; (–■–) $c = 13$ kPa; (_) $c = 0$ kPa.

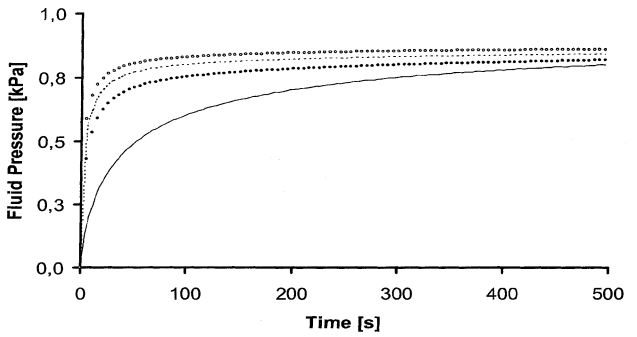

Figure 6. Transient fluid-pressure profile for a constant flow infusion at 0.1 mm^3/min as a function of the viscoelastic modulus c.

(○) $c = 52$ kPa, (– –) $c = 26$ kPa; (●) $c = 13$ kPa; (_) $c = 0$ kPa.

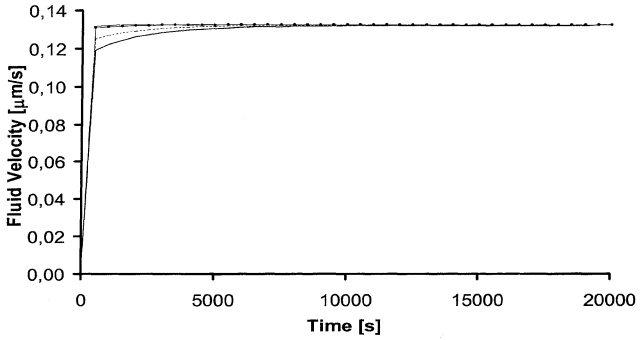

Figure 7. Transient fluid-velocity profile for a constant flow infusion of 0.1 mm^3/min as a function of K.

(_) $K = 7.6 \times 10^{-10}$ m^2/kPa·s; (−−) $K = 3.8 \times 10^{-10}$ m^2/kPa·s; (−·−) $K = 7.6 \times 10^{-11}$ m^2/kPa·s; (−··−) $K = 3.8 \times 10^{-11}$ m^2/kPa·s.

that is, it is only present for time less than τ; at longer times, its effect fades and all the curves fall on the poroelastic one ($c = 0$). The elastic moduli and the hydraulic permeability, K, also contribute to the reduction in evolution time. An increase in the elastic modulus of the matrix results in a faster fluid redistribution within the polymer matrix (data not shown). The transient time is also influenced by the hydraulic conductivity of the matrix; an increase of K leads to a reduction of the transient time, as shown in Figure 7.

Determination of the stress field

From the above analysis it is evident that the fluid flow and pressure distribution differ only from those in a rigid porous material in the transient phase. Therefore, one might conclude that the model is useful only for following phenomena that occur within the transient process. It should be pointed out, however, that the use of poroelastic or poroviscoelastic approaches are also important in the steady-state process, since it allows the evaluation of the solid stress profile within the material. The analysis of the stress field within the material is relevant for an accurate description of the transport processes. Furthermore, the strength of the polymer gel dictates limits on the magnitude of the pressure or of the flow infusion. By calculating the stress distribution within the gel, it is possible to determine the maximum value of the pressure or the flow infusion, which does not cause the polymer network to fail mechanically.

Constant Pressure Infusion. The radial and circumferential (hoop) stresses within the solid matrix resulting from an infusion from a constant pressure source are

$$\sigma_{rr}^{\text{tot}}(r) = \frac{1}{3} PI \cdot a \frac{4r^3 - 6r^2R + 2a^3 + 3\left(\frac{\lambda}{\mu}\right)a^3 - 3\left(\frac{\lambda}{\mu}\right)Ra^2}{(R-a)\left(\frac{\lambda}{\mu}+2\right)r^3} \tag{35}$$

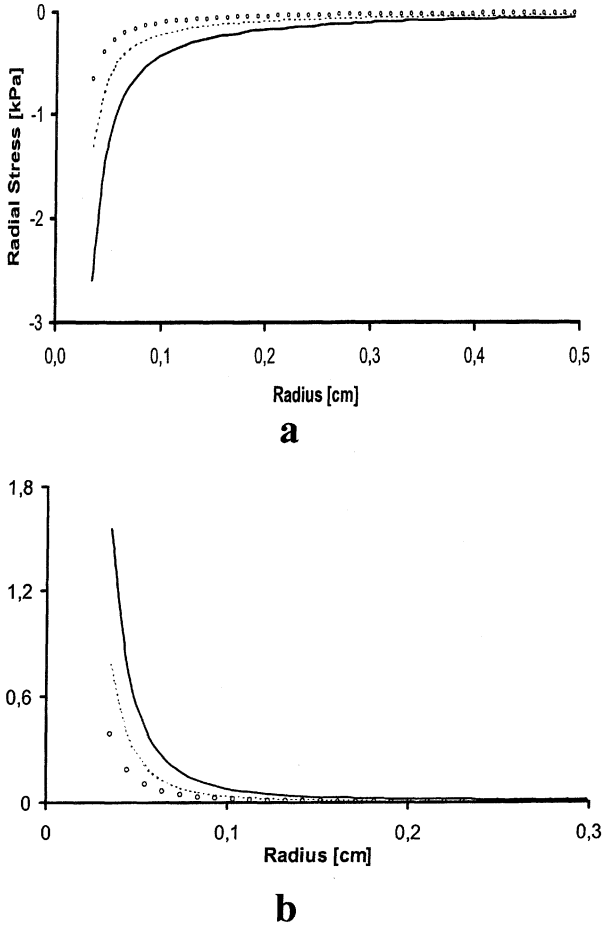

Figure 8. Solid stress profile for a constant pressure infusion.

(a) Radial stress and (b) tangential stress as a function of the infusion pressure. (_) $PI = 2.6$ kPa; (−−) $PI = 1.3$ kPa; (○) $PI = 0.65$ kPa. Note that radial stress is of compression, while tangential stress is of traction.

$$\sigma_{\varphi\varphi}^{\text{tot}}(r) = \sigma_{\theta\theta}^{\text{tot}}(r) = \frac{1}{3} PI \cdot a \frac{-2r^3 + 2a^3 + 3\left(\frac{\lambda}{\mu}\right)a^3 - 3\left(\frac{\lambda}{\mu}\right)Ra^2}{\left(\frac{\lambda}{\mu}+2\right)(a-R)r^3} \tag{36}$$

The stress distribution depends on the infusion pressure and on the elastic modulus of the matrix. Figure 8a shows the steady-state radial-stress profile for different values of the infusion pressure. The radial stress is always negative (compression), with the highest value attained at the solid–liquid interface where the solid stress is equal to the infusion pressure. Figure 8(b) shows the distribution of circumferential stresses at different values of the infusion pressure. The circumferential stress is positive (tension) and, as in the case of the radial stress, the highest value is attained at the solid–liquid interface. It should be noted that while the profile of material dilatation depends on the sum of the Lamè constant ($2\mu + \lambda$), the solid-stress profiles depend on their ratio (λ/μ).

Constant Flow Infusion. The radial and circumferential stresses resulting from an infusion from a constant flow source are

$$\sigma_{rr}^{\text{tot}}(r) = \frac{1}{12}\varphi \cdot Q \frac{4r^3 - 6r^2R + 2a^3 - 3a^2R\left(\frac{\lambda}{\mu}\right) + 3a^3\left(\frac{\lambda}{\mu}\right)}{K\pi\left(\frac{\lambda}{\mu} + 2\right)Rr^3} \tag{37}$$

$$\sigma_{\varphi\varphi}^{\text{tot}} = \sigma_{\theta\theta}^{\text{tot}} = -\frac{1}{12}\varphi \cdot Q \frac{-2r^3 + 2a^3 - 3\left(\frac{\lambda}{\mu}\right)Ra^2 + 3\left(\frac{\lambda}{\mu}\right)a^3}{K\pi\left(\frac{\lambda}{\mu} + 2\right)Rr^3} \tag{38}$$

The stress profiles are dependent on the infusion flow rate, the elastic moduli of the matrix, as well as the fluid flow resistance. Unlike the case of constant pressure infusion, the hydraulic permeability strongly affects the value of the stress, as shown in Figures 9a and 9b. The figures have been expanded around the infusion area to highlight the effect of the hydraulic conductivity and flow rate on the stress distribution. The curves simulate the radial and circumferential stress distribution at three different flow rates (0.1, 1, and 10 mm^3/min) and for two different values of hydraulic conductivity (7.6×10^{-11} and 7.6×10^{-12} $m^2/kPa\cdot s$). At a given flow rate the stress level at the infusion site is controlled by the hydraulic conductivity of the matrix. Therefore, the value of K fixes the maximum flow rate that can be used to avoid the mechanical failure of the matrix. Generally, for polymeric gels or tissues, the load-bearing capability in compression is higher than in tension. Therefore, it is expected that the tangential stress will cause gel breaking more than the radial stress. This should be taken into account for the optimization of an infusion protocol, in order to prevent a mechanical failure of the polymeric gel or tissue.

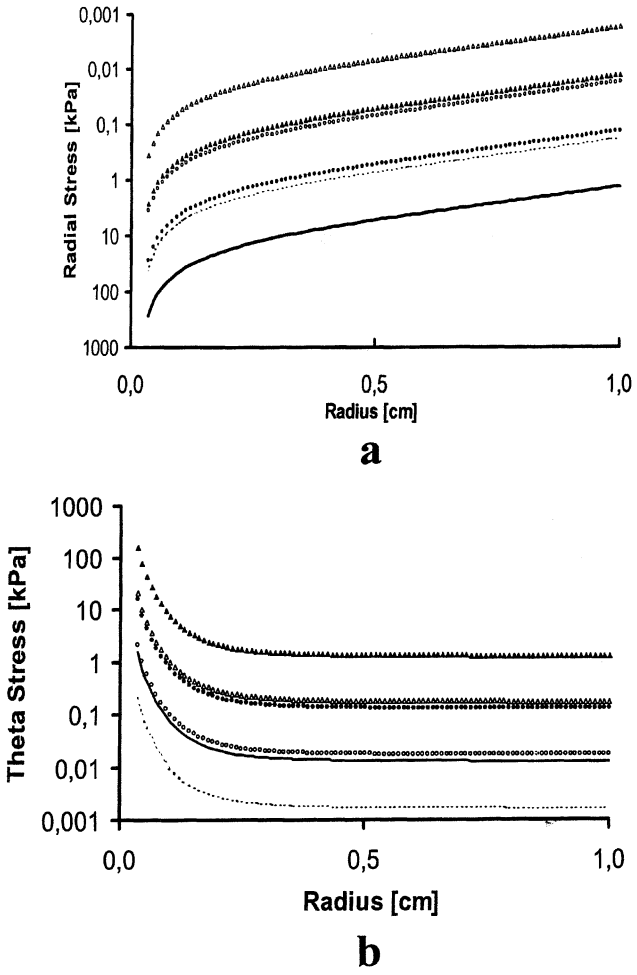

Figure 9. Solid stress profiles, (a) radial stress and (b) tangential stress, for a constant flow infusion, parametric with the infusion flow.

Closed symbols refer to $K = 7.6\times10^{-12}$ $m^2/kPa\cdot s$; open symbols refer to $K = 7.6\times10^{-11}$ $m^2/kPa\cdot s$.

Macromolecular solute distribution

The distribution of macromolecular solutes resulting from an infusion depends on mechanical and hydraulic conductivity parameters, as well as on the diffusion coefficient of the solute within the polymeric matrix. In the following section the role of these parameters on the distribution of a macromolecular solute will be discussed.

Constant Flow Infusion. At a given flow rate, the distribution of macromolecules within the polymer gel depends on the diffusion coefficient, as shown in Figure 10. Since the instantaneous flow of macromolecules entering the gel is given by the product ($Q\ C_o$), the total number of macromolecules within the gel at a given time is the same for all cases. The diffusion mechanism tends to reduce the concentration gradient, and, therefore, for high diffusion coefficients, the concentration profile is smooth over the radius of the gel (Figure 10a). As the diffusion coefficient decreases, the transport becomes convection driven and the concentration profile becomes sharper (Figures 10b and 10c). In the limit for $D \to 0$, the concentration profile is stepwise (Figure 10c).

At short times, the concentration profiles show a surplus, that is, the concentration in the region close to the infusion site exceeds the infusion concentration C_o. This effect becomes more pronounced as the diffusion coefficient decreases, and disappears at longer times when the fluid velocity reaches the steady state. The excess in concentration is due to the nonzero divergence of the velocity field during the transient time. Indeed, the mass balance for the solute (Eq. 18) can be rewritten as

$$\frac{\partial C}{\partial t} = D\nabla^2 C - C\chi\nabla\cdot\boldsymbol{v} - \chi\boldsymbol{v}\cdot\nabla C \tag{39}$$

If the diffusive transport is negligible with respect to the convective one, the time derivative concentration ($\partial C/\partial t$), always positive in sign, is dependent on the convection term ($-(C\chi\nabla\cdot\boldsymbol{v} + \chi\boldsymbol{v}\cdot\nabla C)$). Once the steady state is reached, the divergence of the fluid velocity is zero ($\nabla\cdot\boldsymbol{v} = 0$), so the sign

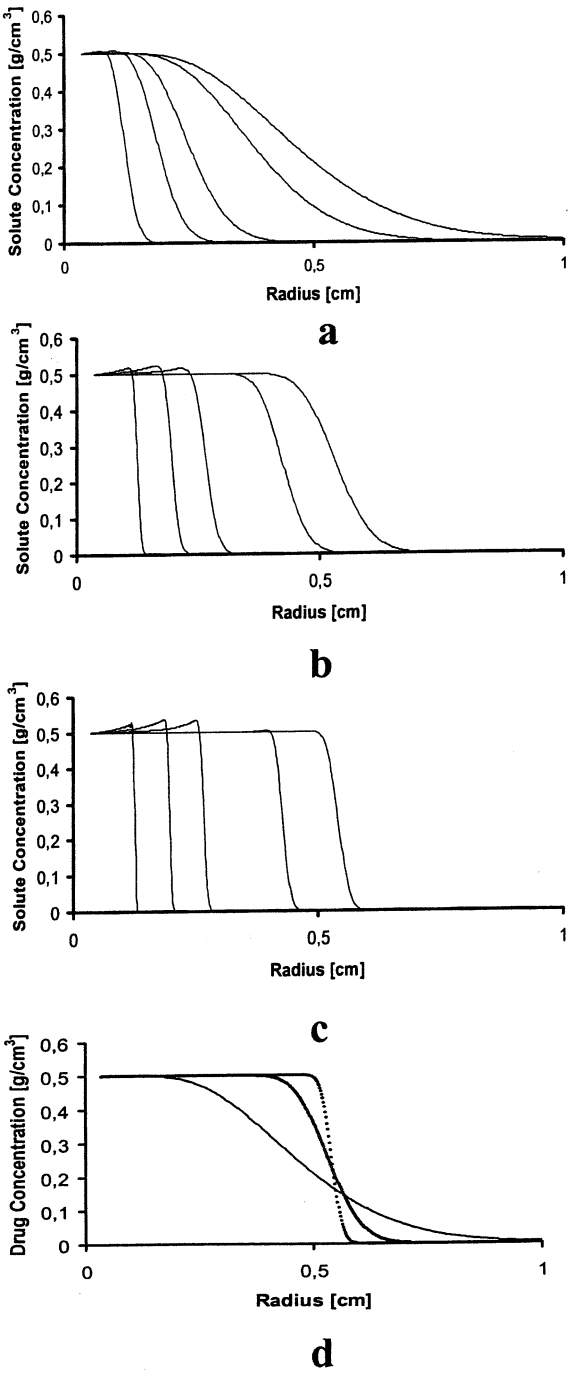

Figure 10. Influence of diffusivity on solute concentration profile for a constant flow infusion at 1 μL/min.

Macromolecular concentration profiles at several times for (a) $D = 1\times10^{-6}$ cm^2/s; (b) $D = 1\times10^{-7}$ cm^2/s; (c) $D = 1\times10^{-8}$ cm^2/s; (d) Comparison among different profiles 11 h after infusion, where (_) $D = 1\times10^{-6}$ cm^2/s; (○) $D = 1\times10^{-7}$ cm^2/s; (●) $D = 1\times10^{-8}$ cm^2/s.

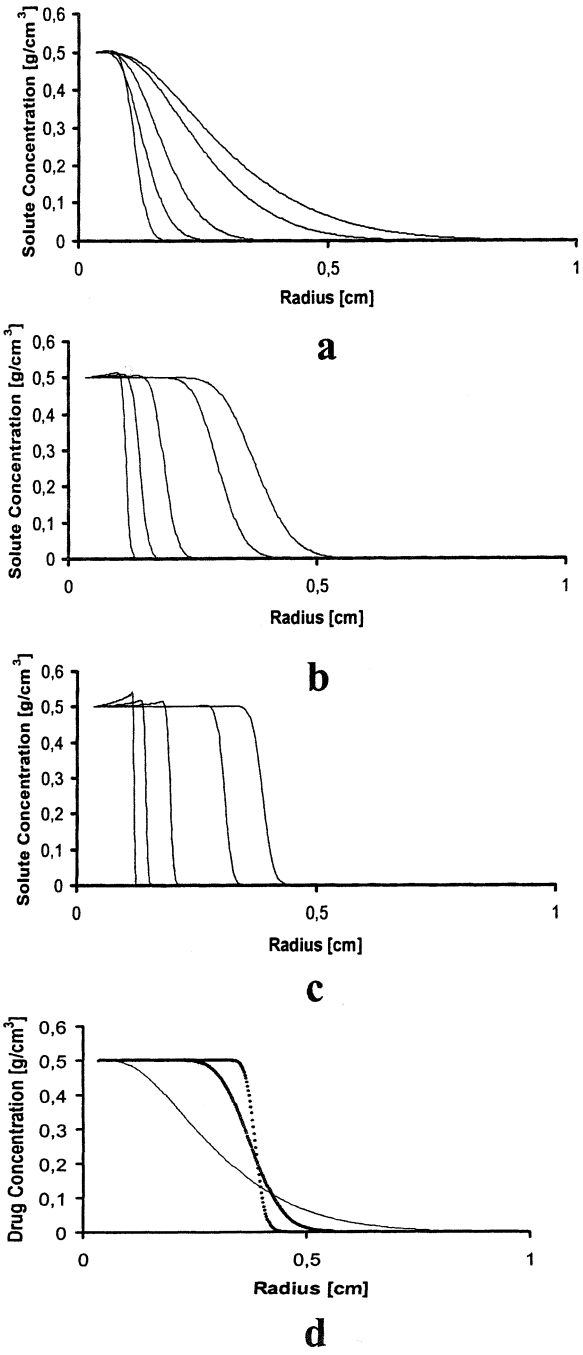

Figure 11. Influence of diffusivity on solute concentration profile for a constant pressure infusion at 10 mmHg.

Macromolecular concentration profiles at several times for (a) $D = 1\times10^{-6}$ cm^2/s; (b) $D = 1\times10^{-7}$ cm^2/s; (c) $D = 1\times10^{-8}$ cm^2/s. (d) Comparison among different profiles 11 h after infusion. (_) $D = 1\times10^{-6}$ cm^2/s; (○) $D = 1\times10^{-7}$ cm^2/s; (●) $D = 1\times10^{-8}$ cm^2/s.

of the concentration gradient (∇C) has to be negative. On the other hand, during the transient phase, the divergence of the fluid velocity is negative and this may lead to a positive value of the concentration gradient, as shown in Figure 10c. In this case, there is a net macromolecular flux against a concentration gradient. At longer times, when the fluid velocity reaches the steady state, the concentration profile flattens out as a consequence of the vanishing fluid-velocity divergence. The same explanation holds when the diffusion term is not

negligible compared to the convection term, although the diffusion mechanism tends to smoothen the concentration excess, as shown in Figure 10a.

Figure 10d shows the effect of the diffusion coefficient on the macromolecular distribution within the gel after 11 h of infusion. As the diffusion coefficient decreases, the profile becomes much sharper, with an abrupt change in correspondence of a given section.

Constant Pressure Infusion. Similar qualitative results are obtained for an infusion from a constant pressure source, shown in Figure 11. Also in this case, as the transport becomes convection driven, the concentration profile becomes sharper. The main differences in the concentration distribution resulting from a constant pressure infusion and a constant flow infusion are due to the fluid-velocity distribution obtainable from the two modality of infusion. These differences were discussed in the previous sections.

Limits of the analysis

The mathematical model presented here allows a unified approach to describe the mechanical behavior of spongelike systems, such as polymeric gels, and the fluid and macromolecular transport. However, this model is based on several simplifying hypotheses. First of all, the model considers a system subjected to small deformations, which allows the use of linear elasticity and viscoelasticity for the solid matrix. Furthermore, it is assumed that the hydraulic permeability, K, is not a function of the gel dilatation. There is experimental evidence indicating that K strongly depends on φ (Tokita and Tanaka, 1991; Johnson, 1996), and this functionality should be included to more accurately describe the fluid transport problem within the gel (Jackson and James, 1982; Mow et al., 1980). However, within the limits of small deformations, the assumption of constant hydraulic permeability does not lead to appreciable errors.

Discussion

The mathematical model presented here describes the fluid and macromolecular transport within polymer gels and its coupling with the mechanical deformation of the polymer matrix. The analysis indicates that either fluid and macromolecular transport or mechanical deformation redistribution is governed by parabolic equations. The characteristic times, associated with the several phenomena involved in the process, arise naturally when we consider the phenomena just discussed as diffusion-like processes.

Fluid transport

The fluid redistribution is regulated by Eq. A4, which can be rewritten as

$$\frac{\partial e}{\partial t} = \left(K(\lambda + 2\mu) + \frac{2cK\int_{-\infty}^{t} m(t-\xi)\frac{\partial}{\partial \xi}(\nabla^2 e)\, d\xi}{\nabla^2 e} \right) \nabla^2 e = Ds(t)\nabla^2 e \quad (39)$$

where $Ds(t)$ assumes the physical meaning of a time-dependent pseudodiffusion coefficient that regulates the rate of matrix dilatation, and, thus, fluid redistribution within the polymer gel. Equation 39 is mathematically similar to those proposed to describe anomalous diffusion generally observed in polymer swelling (Del Nobile, 1994). According to this analogy, the transient fluid redistribution is regulated by the mechanism of fluid percolation through the polymer network and by the configurational relaxation of polymer chains. The mechanism of matrix dilatation redistribution can be *elastic* if the relaxation time is very short or very long compared to the fluid percolation time. Indeed, if the relaxation time, τ, tends to zero, then from Eq. 39 we can see that the pseudodiffusion coefficient Ds becomes equal to $(K(\lambda + 2\mu))$; on the other hand, if $\tau \to \infty$ the pseudodiffusion coefficient $Ds(t)$ tends to $(K\ (\lambda + 2\mu + c))$. In both cases the rate of solid matrix dilatation distribution is not time dependent and depends exclusively on the instantaneous elastic modulus of the solid matrix. When τ is not extremely short or extremely long compared to the percolation time, then the matrix-dilatation redistribution process is defined as *viscoelastic*, and the pseudodiffusion coefficient $Ds(t)$, that is, the rate of the process, is time dependent. To evaluate whether the process of matrix dilatation distribution follows an *elastic* or *viscoelastic* mechanism, it is useful to define the Deborah number for the percolation as the ratio between the relaxation time τ and the percolation time

$$De_{\text{percolation}} = \frac{\tau}{4\pi R^2 / K(\lambda + 2\mu)} \quad (40)$$

The process of fluid redistribution is *elastic* if $De_{\text{percolation}}$ is much less or much greater than unity, while it is *viscoelastic* if $De_{\text{percolation}}$ is close to one.

Macromolecular transport

The distribution of macromolecules resulting from an infusion of fluid within a polymer gel depends, in general, on the transport parameters of the matrix as well as on its mechanical properties. Indeed, if the gel is infused with a solution of a given concentration of macromolecules, the transitory redistribution of fluid throughout the material may have an influence on the distribution of macromolecules. This occurs when the transient time for fluid redistribution is within the same time scale as the macromolecular transport. To establish whether the transient distribution of fluid or matrix dilatation influence the macromolecular distribution within the material, it is useful to compare the time scale for fluid percolation and for the macromolecular transport. The ratio of these two characteristic times, which has a physical meaning similar to the Deborah's number defined earlier, discriminates among several cases that may be occurring

$$De^D = \frac{T_{\text{percolation}}}{\tau_d} \quad (41)$$

For $De^D \gg 1$ or $De^D \ll 1$, the macromolecular concentration profile is not influenced by the transient fluid redistribution, and the transport of macromolecules occurs as if the medium were rigid. On the other hand, if $De^D \approx 1$, the fluid percolation and the macromolecular transport occur within the same

time scale. In this case, the transient evolution of the fluid velocity can influence the distribution of macromolecules, as shown in Figures 10 and 11. The surpluses in concentration shown at times right after infusion, are due to the transient evolution of the fluid velocity profiles. However, this effect vanishes at later times as the velocity profile approaches the steady state. Generally, for polymer gels and biological soft tissue, the time scale for fluid percolation is faster than the diffusion time, and thus the effect of transient fluid distribution, if any, is expected only at early times.

A particular case of transport is expected when the $De^{\text{percolation}} < 1$ (viscoelastic case) and the characteristic time of diffusion are shorter than those of polymer relaxation ($\tau_d < \tau$). This case would be similar to the two-stage diffusion reported for the swelling of polymer gel (Joshi and Astarita, 1979). The diffusion proceeds as a multistage process. In the first stage the diffusion occurs while the solid matrix is undisturbed; later, the solid matrix begins to relax, inducing a different diffusive regime due to the time-evolving dilatation of the gel.

At the steady state of the fluid redistribution, the molecular transport is controlled by two characteristic times: the diffusion time, τ_d, and the convection time, τ_c. The former is given by

$$\tau_d = \frac{\bar{r}^2}{D} \tag{42}$$

where D is the diffusion coefficient and $\bar{r}$ is a characteristic length, which in our case is the radial coordinate. The convection time can be evaluated by

$$\tau_c(\bar{r}) = \int_a^{\bar{r}} \frac{dr}{v(r)} = A(\bar{r}^3 - a^3) \tag{43}$$

where $v(r)$ is the velocity profile, A is a constant that is equal to $[((R-a)/(3Ra)(\varphi/(PI \cdot K))]$ for constant pressure infusion, and $(4\pi/3Q)$ for constant flow infusion. The ratio between the diffusion and convection time, the Peclet's number, indicates which mechanism controls the transport process

$$Pe = \frac{\tau_d}{\tau_c} \tag{44}$$

If $\mathrm{Pe} > 1$, the macromolecular transport occurs mainly by convection, while if $Pe < 1$, diffusion is the dominant transport mechanism. In the case of $Pe \approx 1$, both mechanisms control the distribution of macromolecules within the material. In the case studied here, Pe is a decreasing function of the radial coordinate, and, thus, there may be a switch from a convection-controlled transport, occurring in the region close to the infusion site, to a diffusion-controlled transport, occurring in the region far from the infusion site. The radial position, $\bar{r}$, at which this switch occurs is evaluated by imposing $Pe = 1$, that is

$$Pe = \frac{\tau_d}{\tau_c} = \frac{AD(\bar{r}^3 - a^3)}{\bar{r}^2} = 1 \tag{45}$$

The concentration profile will advance with the typical step shape of a convection-controlled transport, until the section of coordinate, $\bar{r}$, where it will switch to a sigmoidal shape typical of diffusive transport. The coordinate $\bar{r}$ decreases as D increases, as shown in Figures 10 and 11. Therefore, given the transport properties of a polymer gel, $\bar{r}$ is a measure of the maximum radial position that can be loaded with a constant concentration of macromolecules.

The depth of penetration, $\bar{\bar{r}}$ of the macromolecules within the gel at a given time, T, after infusion, can be evaluated assuming that convection and diffusion mechanisms occur in parallel (Levenspiel, 1972), that is

$$\frac{1}{T} = \frac{1}{\tau_c} + \frac{1}{\tau_d} \tag{46}$$

Expressing Eq. 46 in terms of the Peclet number, we have

$$T = \frac{1}{1 + Pe(\bar{\bar{r}})}\tau_d \tag{47}$$

from which the penetration depth, $\bar{\bar{r}}$, can be easily evaluated.

Implications for tissue regeneration and drug delivery

Polymeric hydrogels have been largely used as growth-factor delivery systems to regenerate tissues and organs (Shea et al., 1999; Baldwin and Saltzman, 1998; Jen et al., 1996). Generally these devices are engineered to operate under mechanically static conditions. However, to regenerate tissues, such as bone, muscles, blood vessels, and cartilage, and in engineering bioreactors such as cell-seeded scaffolds, these systems have to work in a mechanically dynamic environment, and this might alter their delivery mechanism significantly (Kim et al., 1999; Niklason et al., 1999). Recently, mechanically activated delivery gels have been proposed as novel intelligent devices to guide tissue formation in a complex stressed environment (Lee et al., 2000). The model presented here, which couples the mechanical deformation with the transport of macromolecules within a polymer gel, provides a useful tool for engineering polymer matrices for such applications. Furthermore, a critical problem often encountered in the use of polymer gels as drug delivery matrices is the optimization of the technique to load the bioactive molecule (Anseth et al., 1996). There are two main approaches to loading a bioactive molecule within a polymer gel: (1) to mix the bioactive molecule in the gel precursor solution and let the gel form, and (2) load the formed gel by soaking it in a solution containing the bioactive molecule. The former approach can be used when the gelling conditions are permissible for biomolecule activity, such as in the case of thermo- or ionic-induced gelation. For gels that are formed in conditions that are not compatible with the activity of the biomolecule, such as in the case of chemically cross-linked gels, the latter approach must be used. In that case, since the loading process relies mainly on diffusion, it may require a very long time to achieve equilibrium. To circumvent this limitation, a convection-enhanced loading process can be followed by microinjecting or perfusing the drug through the gel. For these kinds

of approaches, the model presented here may be very helpful in designing and controlling the gel loading process.

Interstitial movement of fluids and macromolecules is part of a complex equilibrium between the fluid pressures and tissue stresses and deformation. The control and prediction of the macromolecular distribution that follows a direct tissue infusion is of relevant interest in diagnosis and therapy (Bobo et al., 1994; Boucher et al., 1998; Jain, 1994). The model presented here can be used as an optimization tool for direct infusion in living tissue, such as those performed for diagnostic (such as lymphagiography) as well as therapeutic reasons. Intratumoral injection, for example, has recently received interest as a means of circumventing the transport barriers for delivery of macromolecules such as antibodies, DNA fragments, or viruses (Bobo et al., 1994.; Morrison et al., 1994, Boucher et al., 1998), since it has been shown that direct intratumoral infusion can enhance drug concentrations by orders of magnitude compared to those achieved by systemic delivery (Morrison et al., 1994; Bobo et al., 1994). In these applications, and in particular for intratumoral infusion, the goal is to deliver the maximum amount of drug in the shortest time and, most importantly, distributed as uniformly as possible throughout the tissue (Boucher et al., 1998; Bobo et al., 1994; McGuire and Yuan, 2001). However, these two goals are often opposite to each other. Indeed, infusing at an elevated flow rate would guarantee a high delivery rate, on the one hand, but a probable tissue rupture due to elevated solid stress and, therefore, a nonuniform drug distribution, on the other hand. Previous attempts to describe macromolecular distributions within the tumor mass have not considered the role of the coupling tissue mechanics and transport (Morrison et al., 1994). Thus, the optimizing of an infusion protocol has to take into account the complex relationship that exists between the transport phenomena and its coupling with tissue mechanics. An application of the model presented here for predicting and controlling the macromolecular distribution that results from direct infusion within a tumor mass and the guidelines for optmization intratumoral infusion protocol based on tissue mechanics is currently ongoing and will be the subject of a future article. Several alternatives to infusing a tumor tissue in order to prevent fluid leakage due to rupture of the system and to enhance and improve drug distribution within a solid tumor will be presented and critically discussed. Since during single-point infusion the most stressed area is at the infusion cavity, the use of multiple infusion sources and injecting smaller amounts of macromolecular solution could prevent tissue damage and, at the same time, ensure a higher delivery rate. As an alternative, better distribution can be obtained by oscillating flow rates of drug-solution infusion, exploiting the transient of the solid stress field. Aside from the applications mentioned herein, the model is also useful for several other cases in the fields of bioreactor design, food technology, and tissue engineering.

Conclusion

The model presented herein, although with some simplifying assumptions, provides new insight into understanding the coupling between mechanics and transport in soft hydrated gels. It can be used to design and engineer novel drug delivery systems, which have to operate in a mechanically dynamic environment, as well as optimizing a drug delivery protocol to be used in therapy and diagnostics. Furthermore, the model represents a useful tool for experimentally evaluating the transport and mechanical parameters of soft hydrated gels and tissues.

The results obtained are physically sound and show transient phenomena in the macromolecular distribution following an infusion from a constant flow or pressure source that is not predictable by a rigid porous or by a poroelastic model. These results, once experimentally confirmed, can be further exploited to formulate novel approaches that may help in enhancing macromolecular distribution within gels and tissues. These approaches include oscillating infusion pressure or flow as well as periodic mechanical deformation of the solid matrix.

Furthermore, the model also predicts the evolution of the stress field within the solid matrix. This aspect is very important, since polymer gels, especially physically reversible gels, are vulnerable to tension breakage. Mechanical failure of the gel leads to the formation of fluids and solutes channeling, and, therefore, impair a uniform distribution of macromolecules within the polymer matrix.

Acknowledgment

This work was supported in part by the Italian Minister of Scientific Research (MUIR) and the National Cancer Institute (NCI). The authors gratefully acknowledge Dr. Fabrizio Sarghini for helping with the finite-element analysis and Dr. Francesco Mollica for helpful discussions and careful proofreading of the article.

Notation

a = internal radius of the sphere, cm
c = viscoelastic modulus, kPa
C = macromolecular solute concentration, g/cm^3
C^i = macromolecular solute concentration in the gel interface, g/cm^3
C^* = macromolecular solute concentration in the cavity, g/cm^3
D = diffusion coefficient, cm^2/s
Ds = pseudodiffusion coefficient, cm^2/s
e = solid matrix dilatation
f = frictional coefficient
$\boldsymbol{F}_a$ = frictional force, N
H = spectrum of relaxation-time function
K = hydraulic permeability, m^2/kPa·s
N_c, N_d = convective and diffusive macromolecular concentration fluxes, g/cm^2·s
p = fluid pressure, kPa
PI = infusion pressure, kPa
Q = infusion flow, mm^3/min
r = spatial coordinate, cm
R = external radius of the sphere, cm
$T_{\text{percolation}}$ = percolation time, s
$\boldsymbol{u}$ = solid matrix displacement, μm
$\boldsymbol{v}$ = fluid velocity, μm/s
V = volume of the gel, cm^3
V_o = undeformed volume of the gel, cm^3
V^f, V_o^f = fluid volume in deformed and undeformed state of the gel, cm^3

Greek letters

δ = semiamplitude of the relaxation-time spectrum, s
$\underline{\underline{\boldsymbol{\epsilon}}}$ = solid deformation tensor
χ = screening coefficient
ϕ = solubility coefficient
φ = volumetric fluid fraction

λ, μ = Lamè constants for solid matrix, kPa
$\mathbf{\Pi}$ = sum of the external forces acting on the single phase, N
ρ_f, ρ_s = fluid- and solid-phase density, g/cm^3
$\underline{\underline{\sigma}}^s$, $\underline{\underline{\sigma}}^f$ = solid- and fluid-phase stress tensor, kPa
τ = viscoelastic relaxation time, s
τ_c, τ_d = convective and diffusive characteristic time, s

Literature Cited

Anseth, K. S., C. N. Bowman, and L. Brannon-Peppas, "Mechanical Properties of Hydrogels and their Experimental Determination," *Biomaterials*, **17**, 1647 (1996).

Ateshian, G. A., W. H. Warden, J. J. Kim, R. P. Grelsamer, and V. C. Mow, "Finite Deformation Biphasic Material Properties of Bovine Articular Cartilage from Confined Compression Experiments," *J. Biomech.*, **30**, 1157 (1997).

Baldwin, S. P., and W. M. Saltzman, "Materials for Protein Delivery in Tissue Engineering," *Adv. Drug Delivery Rev.*, **33**, 71 (1998).

Biot, M. A., "The Theory of Elasticity and Consolidation for a Porous Anisothropic Solid," *J. Appl. Phys.*, **12**, 155 (1941).

Biot, M. A., "Theory of Elasticity and Consolidation for a Porous Anisotropic Solid," *J. Appl. Phys.*, **26**, 186 (1955).

Bobo, R. H., D. W. Laske, A. Akbasak, P. F. Morrison, R. L. Dedrick, and E. H. Oldfield, "Convection-Enhanced Delivery of Macromolecules in the Brain," *Proc. Natl. Acad. Sci. USA*, **91**, 2076 (1994).

Boucher, Y., C. Brekken, P. A. Netti, L. T. Baxter, and R. K. Jain, "Intratumoral Infusion of Fluid: Estimation of Hydraulic Conductivity and Implications for the Delivery of Therapeutic Agents," *Br. J. Cancer*, **78**, 1442 (1998).

Del Nobile, M. A., G. Mensitieri, P. A. Netti, and L. Nicolais, "Anomalous Diffusion in Poly-Ether-Ketone," *Chem. Eng. Sci.*, **49**, 633 (1994).

Doi, M., "Stress-Diffusion Coupling," *Proc. Int. Congr. on Rheology* (1996).

Doi, M., and S. F. Edwards, *The Theory of Polymer Dynamics*, Clarendon, Oxford (1986).

Flory, P. J., *Principles of Polymer Chemistry*, Cornell Univ. Press, Ithaca, NY (1992).

Frank, E. H., and A. J. Grodzinsky, "Cartilage Electromechanics: II. A Continuum Model of Cartilage Electrokinetic and Correlation with Experiments," *J. Biomech.*, **20**, 629 (1987).

Fung, Y. C., *Biomechanics: Motion, Flow, Stress and Growth*, Springer-Verlag, New York (1990).

Hoog, F. R., J. H. Knight, and A. N. Stokes, "An Improved Method for Numerical Inversion of Laplace Transforms," *SIAM J. Sci. Stat. Comput.*, **3**, 357 (1982).

Ianniruberto, G., F. Greco, and G. Marrucci, "The Two-Fluid Theory of Polymer Migration in Slit Flow," *Ind. Eng. Chem. Res.*, **33**, 2404 (1994).

Jackson, G. W., and D. F. James, "The Hydrodynamic Resistance of Hyaluronic Acid and Its Contribution to Tissue Permeability," *Biorheology*, **19**, 317 (1982).

Jain, R. K., "Barriers to Drug Delivery in Solid Tumors," *Sci. Amer.*, **271**, 58 (1994).

Jain, R. K., "Transport of Molecules in the Tumor Interstitium: A Review," *Cancer Res.*, **47**, 3038 (1987).

Jen, A. C., M. C. Wake, and A. G. Mikos, "Hydrogel for Cell Immobilization," *Biotechnol. Bioeng.*, **50**, 357 (1996).

Johnson, E. M., and W. M. Deen, "Hydraulic Permeability of Agarose Gel," *AIChE J.*, **42**, 5 (1996).

Johnston, S. T., and W. M. Deen, "Hindered Convection of Proteins in Agarose Gel," *J. Membr. Sci.*, **153**, 271 (1999).

Joshi, S., and G. Astarita, "Diffusion-Relaxation Coupling in Polymers Which Show Two-Stage Sorption Phenomena," *Polymer*, **20**, 455 (1979).

Kim, B. S., J. Nikolovsky, J. Bonadio, and D. J. Mooney, "Cyclic Mechanical Strain Regulates the Development of Engineered Smooth Muscle Tissue," *Nat. Biotechnol.*, **17**, 979 (1999).

Lee, K. Y., M. C. Peters, K. W. Anderson, and D. J. Mooney, "Controlled Growth Factor Release from Synthetic Extracellular Matrices," *Nature*, **408**, 998 (2000).

Levenspiel, O., *Chemical Reaction Engineering*, Wiley, New York (1972).

McGuire, S., and F. Yuan, "Quantitative Analysis of Intratumoral Infusion of Color Molecules," *AJP Heart Circ. Physiol.*, **251**, 715 (2001).

Macosko, C. W., *Rheology Principles, Measurements and Applications*, Wiley-VCH, New York (1994).

Mak, A. F., "The Apparent Viscoelastic Behaviour of Articular Cartilage—The Contributions from Intrinsic Matrix Viscoelasticity and Interstitial Flow," *J. Biomech. Eng.*, **108**, 123 (1986).

Morrison, P. F., D. W. Laske, R. H. Bobo, E. H. Oldfield, and R. L. Dedrick, "High Flow Microinfusion: Tissue Penetration and Pharmacodynamics," *Amer. J. of Physiol.*, **266**, 292 (1994).

Mow, V. C., M. K. Kwan, W. M. Lai, and C. G. Armstrong, "A Finite Deformation Theory for Nonlinearly Permeable Soft Hydrated Biological Tissues," *Frontiers in Biomechanics*, G. Schmid-Schonbein, L.-Y. Woo, and B. W. Zweifach, eds., Springer-Verlag, New York (1986).

Mow, V. C., S. C. Kuei, W. M. Lai, and C. G. Armstrong, "Biphasic Creep and Stress Relaxation of Articular Cartilage in Compression: Theory and Experiments," *J. Biomech. Eng.*, **102**, 73 (1980).

Muhr, A. H., and J. M. V. Blanshard, "Diffusion in Gel," *Polymer*, **23**, 1012 (1982).

Netti, P. A., L. T. Baxter, and Y. Boucher, "Macro and Microscopic Fluid Transport in Living Tissues: Application to Solid Tumors," *AIChE J.*, **43**, 3 (1997).

Netti, P. A., D. A. Berk, M. A. Swartz, A. J. Grodzinsky, and R. K. Jain, "Role of Extracellular Matrix Assembly in Interstitial Transport in Solid Tumors," *Cancer Res.*, **60**, 2497 (2000).

Nicholson, C., and J. M. Phillips, "Ion Diffusion Modified by Tortuosity and Volume Fraction in the Extracellular Environment of Rat Cerebellum," *J. Physiol.*, **321**, 225 (1981).

Niklason, L. E., J. Gao, W. M. Abbot, K. K. Hirschi, S. Houser, R. Martini, R. Langer, "Functional Arteries Growth in Vitro," *Science*, **284**, 489 (1999).

Shea, L. D., E. Smiley, J. Bonadio, J., and D. J. Mooney, "DNA Delivery from Polymeric Matrices for Tissue Engineering," *Nat. Biotechnol.*, **17**, 551 (1999).

Swabb, E. A., J. Wei, and P. M. Gullino, "Diffusion and Convection in Normal and Neoplastic Tissues," *Cancer Res.*, **34**, 1214 (1974).

Tokita, M., and T. Tanaka, "Friction Coefficient of Polymer Networks of Gel," *J. Chem. Phys.*, **95**, 6 (1991).

Truesdell, C., and R. A. Toupin, "The Classical Field Theory," *Handbuck der Physik*, Vol. II/I, Sprinter, Berlin (1960).

Appendix A: Application of the Model to a Spherical Geometry

In this section we will derive the equations that describe the mechanics of a polymeric gel, by combining the mass and momentum balances for the fluid and solid phase and reduce them for a spherical geometry.

For a spherical geometry, the following relationships hold

$$\nabla\cdot\underline{\underline{\varepsilon}} = \frac{1}{2}\nabla\cdot\nabla\boldsymbol{u}_r + \frac{1}{2}\nabla e$$

$$\nabla e = \nabla\cdot\nabla\boldsymbol{u}_r$$

$$\nabla\cdot\nabla e = \nabla^2 e$$

$$\nabla\cdot(\nabla\cdot\nabla\boldsymbol{u}_r) = \nabla^2 e \qquad \text{(A1)}$$

Combining the momentum balance for the solid–fluid system (Eq. 7) and the constitutive equation for the solid matrix (Eq. 8) leads to

$$\nabla^2 p = (\lambda + 2\mu)\nabla^2 e + 2c\int_{-\infty}^{t} m(t-\xi)\frac{\partial}{\partial\xi}(\nabla^2 e)\, d\xi \qquad \text{(A2)}$$

From the continuity equation (Eq. 3) and Eq. 12, we have

$$K\nabla^2 p = \nabla\cdot\frac{\partial}{\partial t}u_r \tag{A3}$$

and substituting Eq. A3 in Eq. A2 and considering that the divergence of the displacement field is the dilatation field, we have

$$\frac{\partial e}{\partial t} = K(\lambda+2\mu)\nabla^2 e + 2cK\int_{-\infty}^{t} m(t-\tau)\frac{\partial}{\partial\xi}(\nabla^2 e)\,d\xi \tag{A4}$$

To transform Eq. A4 in the Laplace space, let us first evaluate the transform of the memory function (Eq. 9):

$$\hat{m}(s) = \frac{1}{s}\frac{\tau}{\delta}\ln\left(\frac{s(\tau+\delta)+1}{s(\tau-\delta)+1}\right) \tag{A5}$$

The integral term in Eq. A4 is a convolution integral. Using the result of Eq. A5, and so transforming Eq. A4, we have

$$s\hat{e}(s,r) - e(0,r) = K(\lambda+2\mu)\frac{1}{r^2}\frac{\partial}{\partial r}\left(r^2\frac{\partial\hat{e}(s,r)}{\partial r}\right) + \frac{2c\tau}{\delta}\ln\left(\frac{s(\tau+\delta)+1}{s(\tau-\delta)+1}\right)\frac{1}{r^2}\frac{\partial}{\partial r}\left(r^2\frac{\partial\hat{e}(s,r)}{\partial r}\right) \tag{A6}$$

If the gel is initially in the undeformed state (that is, $e(0,r) = 0$), Eq. A6 is a modified Bessel equation in spherical coordinates, and its general solution is

$$\hat{e}(s,r) = \frac{A\sinh(r\alpha)}{r\alpha} + \frac{B\cosh(r\alpha)}{r\alpha} \tag{A7}$$

where α is a complex parameter function of the characteristic material parameters

$$\alpha^2 = \frac{s}{K\left[(\lambda+2\mu) + \frac{2c\tau}{\delta}\ln\left(\frac{s(\tau+\delta)+1}{s(\tau-\delta)+1}\right)\right]} \tag{A8}$$

Also if the gel is not initially in the undeformed state, Eq. A7 is still a general solution of Eq. A6 expressed in terms of variational variables.

To solve Eq. A7, the boundary conditions need to be specified. In the following section, the boundary conditions for a constant pressure and a constant flow infusion will be derived.

Constant pressure infusion

Equation A4 can be rewritten in the following form

$$\nabla^2 p = \nabla^2\left[(\lambda+2\mu)e + 2c\int_{-\infty}^{t} m(t-\xi)\frac{\partial}{\partial\xi}e\,d\xi\right] \tag{A9}$$

Assuming that the radius of the sphere (R) is sufficiently large compared to the radius of the cavity (a), then we can consider that both the dilatation and its gradient tend to zero as $r \to R$, so

$$\nabla p = \nabla\left[(\lambda+2\mu)e + 2c\int_{-\infty}^{t} m(t-\xi)\frac{\partial}{\partial\xi}e\,d\xi\right] \tag{A10}$$

$$p(t,r) = (\lambda+2\mu)e(t,r) + 2c\int_{-\infty}^{t} m(t-\xi)\frac{\partial}{\partial\xi}e(t,r)\,d\xi \tag{A11}$$

Equation A10 furnishes the boundary condition at $r \to a$

$$PI = (\lambda+2\mu)e(t,a) + 2c\int_{-\infty}^{t} m(t-\tau)\frac{\partial}{\partial\xi}e(t,a)\,d\xi \tag{A12}$$

Transforming Eq. A11 in the Laplace space, we have

$$\hat{e}(s,a) = \frac{PI}{s\left[\lambda+2\mu+\frac{2c\tau}{\delta}\ln\left(\frac{s(\tau+\delta)+1}{s(\tau-\delta)+1}\right)\right]} \tag{A13}$$

With Eq. A13, the solution of Eq. A7 becomes

$$\hat{e}(s,r) = \frac{D(s)a}{r}\frac{\sinh[(R-r)\alpha]}{\sinh[(R-a)\alpha]} \tag{A14}$$

where $D(s) = \hat{e}(s,a)$.

Constant flow infusion

The solid stress acting at the boundary between the fluid and the solid phase is zero; therefore at $r = a$

$$2\mu\underline{\underline{\varepsilon}}(t,a) + \lambda e(t,a)\underline{\underline{I}} + c\int_{-\infty}^{t} m(t-\xi)\frac{\partial}{\partial\xi}\left(\underline{\underline{\varepsilon}}(t,a) + e(t,a)\underline{\underline{I}}\right)d\xi = 0 \tag{A15}$$

Rewriting in spherical coordinates and transforming in the Laplace space, we obtain

$$M(s)\frac{\partial}{\partial r}\hat{u}_r(s,a) + T(s)\hat{e}(s,a) = 0 \tag{A16}$$

where

$$M(s)=\left[2\mu+\frac{c_t}{\delta}\ln\left(\frac{s(\tau+\delta)+1}{s(\tau-\delta)+1}\right)\right]$$

$$T(s)=\left[\lambda+\frac{c\tau}{\delta}\ln\left(\frac{s(\tau+\delta)+1}{s(\tau-\delta)+1}\right)\right] \quad \text{(A17)}$$

The dilatation, e, can be expressed as function of displacement u, as

$$\hat{e}(s,a)=\frac{\partial}{\partial r}\hat{u}_r(s,a)-\frac{2\hat{u}(s,a)}{a} \quad \text{(A18)}$$

Combining Eqs. A16 and A18, we obtain

$$\hat{u}_r(s,a)=\frac{(M(s)+T(s))a_o}{2M(s)}\hat{e}(s,a) \quad \text{(A19)}$$

From Darcy's law, assuming that the cavity radius does not change significantly, at $r=a$ we have

$$\varphi\left(\frac{Q}{4\pi a^2}-\frac{\partial u_r}{\partial t}\right)=-K\nabla p \quad \text{(A20)}$$

Transforming the preceding equation in the Laplace space and substituting Eq. A19, we obtain the boundary condition that links the dilatation to the flow rate at $r=a$

$$\frac{\partial\hat{e}(s,a)}{\partial r}+C(s)\hat{e}(s,a)+D'(s)=0 \quad \text{(A21)}$$

where

$$F(s)=\left[\lambda+2\mu+\frac{2c\tau}{\delta}\ln\left(\frac{s(\tau+\delta)+1}{s(\tau-\delta)+1}\right)\right]$$

$$C(s)=-\frac{a\varphi s}{2KM(s)}$$

$$D'(s)=\frac{\varphi Q}{4K\pi a^2 sF(s)} \quad \text{(A22)}$$

With Eq. A21, the solution of Eq. A7 becomes

$$\hat{e}(s,r)=\frac{D'(s)a^2}{r}\times\frac{\sinh[(R-r)\alpha]}{(1-C(s)a)\sinh[(R-a)\alpha]+\alpha a\cosh[(R-a)\alpha]} \quad \text{(A23)}$$

Once the distribution of $\hat{e}$ is known, all the other variables $\hat{p}$, $\hat{u}$, $\hat{v}$, and $\hat{\sigma}$ can be evaluated.

From Eq. A11, transforming in the Laplace space, the hydrostatic fluid pressure results

$$\hat{p}(s,r)=F(s)\hat{e}(s,r) \quad \text{(A24)}$$

The displacement field is readily obtained by

$$\frac{1}{r^2}\frac{d}{dr}\left(r^2\hat{u}_r\right)=\hat{e} \quad \text{(A25)}$$

Equation (A25) can be solved using the boundary condition

$$\hat{\sigma}_{rr}^{s}(s,a)=A(s)\hat{e}(s,a)+B(s)\frac{d}{dr}\hat{u}_r(s,a)=0 \quad \text{(A26)}$$

where $A(s)$ and $B(s)$ are complex parameters that take into account the characteristic parameters of the material and are obtained by the expression of the solid stress tensor in the complex Laplace space

$$\underline{\underline{\hat{\sigma}}}^{s}=\lambda\hat{e}I+2\mu\underline{\underline{\hat{\varepsilon}}}+\frac{c_t}{\delta}\ln\left(\frac{s(\tau+\delta)+1}{s(\tau-\delta)+1}\right)\left(\underline{\underline{\hat{\varepsilon}}}+\hat{e}\underline{\underline{I}}\right) \quad \text{(A27)}$$

which, rearranged, becomes

$$\hat{\sigma}^{s}=A(s)\hat{e}\underline{\underline{I}}+B(s)\underline{\underline{\varepsilon}} \quad \text{(A28)}$$

where

$$A(s)=\lambda+\frac{c\tau}{\delta}\ln\left(\frac{s(\tau+\delta)+1}{s(\tau-\delta)+1}\right)$$

$$B(s)=2\mu+\frac{c\tau}{\delta}\ln\left(\frac{s(\tau+\delta)+1}{s(\tau-\delta)+1}\right) \quad \text{(A29)}$$

Through the analytical expressions of the hydrostatic pressure and the matrix displacement, it is possible to obtain an expression of the fluid velocity by simply transforming Darcy's equation in the complex Laplace space, that is

$$\hat{v}(s,r)=s\hat{u}_r(s,r)-\frac{K}{\varphi}\frac{\partial\hat{p}(s,r)}{\partial r} \quad \text{(A30)}$$

Here to determine $\boldsymbol{v}$ we assumed that the volumetric fraction of fluid phase φ is constant. In reality, the fluid volume fraction, even assuming small deformation, is a function of the dilatation. Indeed, we express e as

$$e\cong\frac{V_g-V_g^o}{V_g^o} \quad \text{(A31)}$$

where V_g^o and V_g are the undeformed and deformed volumes of the gel. From a fluid mass balance we get

$$V_g^o\varphi^o-V_g\varphi=V_g^o-V_g \quad \text{(A32)}$$

where φ^o and φ are the fluid fractions in the undeformed and deformed state. From Eqs. A31 and A32, the fluid fraction can be obtained as a function of the dilatation as

$$\varphi=\frac{e+\varphi^o}{1+e} \quad \text{(A33)}$$

Once the distribution of e and u are known, the principal components of the stress tensor, along r, θ and φ coordinates, are obtained from the gel constitutive equation

$$\hat{\sigma}^s_{rr}(s, r) = (A(s) - F(s))\hat{e}(s, r) + B(s)\frac{d}{dr}\hat{u}_r(s, r) = 0 \quad \text{(A34)}$$

$$\hat{\sigma}^s_{\theta\theta}(s, r) = \hat{\sigma}^s_{\varphi\varphi}(s, r) = (A(s) - F(s))\hat{e}(s, r) + B(s)\frac{\hat{u}_r(s, r)}{r} = 0 \quad \text{(A35)}$$

Appendix B: Finite-Element Analysis for the Solute Transport Problem

In order to discretize the domain of the field of solute concentration, we will use a partition of the interval Ω in closed segments, whose measure is Ω_i. Each segment constitutes a subdomain. Thus, we can write

$$\Omega = \sum_i \Omega_i(r_i). \quad \text{(B1)}$$

Each function present in the transport equation is defined in the single subdomain, Ω_i. We multiply each term of the equation by a family of linear weight functions, w_i, belonging to the Hilbert space. Each weight function, w_i, is defined in the subdomain, Ω_i, and the value they assume on the border of the domain is zero. Now we can formulate the problem in a weak form with the Galerkin method as follows

$$\sum_i \int_{\Omega_i} w_i \, D\nabla c_i \, d\Omega_i = -\sum_i \int_{\Omega_i} \nabla w_i \, D\nabla c_i \, d\Omega_i \quad \text{(B2)}$$

The Laplacian integral can be transformed by using Stokes' theorem in the following way

$$\sum_i \int_{\Omega_i} w_i \, D\nabla c_i \, d\Omega_i = -\sum_i \int_{\Omega_i} \nabla w_i \, D\nabla c_i \, d\Omega_i \quad \text{(B2)}$$

from which we have

$$\sum_i \int_{\Omega_i} w_i \frac{\partial c_i}{\partial t} d\Omega_i = -\sum_i \int_{\Omega_i} \nabla w_i \, D\nabla c_i \, d\Omega_i - \sum_i \int_{\Omega_i} w_i \nabla\cdot(c_i \chi \nu_i) \, d\Omega_i \quad \text{(B3)}$$

The final step is to integrate each term in Eq. A39.

Manuscript received May 22, 2002, revision received Oct. 30, 2002, and final revision received Dec. 18, 2002.